Saito *et al. Journal of Wood Science* (2023) 69:20
https://doi.org/10.1186/s10086-023-02094-1

Journal of Wood Science

ORIGINAL ARTICLE

Open Access

Influence of hemicellulose and lignin on intermolecular interaction between quinacridone and lignocellulosic fibers revealed by gel-state NMR and color measurements

Yasuko Saito[1*], Keita Sakakibara[1], Yuki Tanaka[2], Naoya Hontama[2] and Takashi Endo[1]

Abstract

Quinacridone, a π-conjugated planar molecule, and common red pigment in industrial and painting applications, easily aggregates to form large clusters of pigment particles, resulting in a reduction in color strength. Cotton-derived cellulose nanofiber (NF), which almost consists of cellulose without hemicellulose and lignin, has been found to adsorb quinacridone on the surface, which inhibits pigment aggregation. The aggregation inhibition property of cellulose NF was induced by the strong intermolecular interactions between cellulose and quinacridone. In this study, the properties of lignocellulosic fibers for suppressing the aggregation of quinacridone pigments were investigated to reveal the influence of hemicellulose and lignin on the intermolecular interactions between quinacridone and fibers. Two lignocellulosic fibers with different degrees of fibrillation were used as dispersants of the pigment. In the scanning electron microscopy (SEM) images of the quinacridone–lignocellulose mixture, quinacridone particles were observed along the lignocellulose fiber, indicating that the quinacridone particles were well-adsorbed on the fiber surface. Consequently, the color of the aqueous suspension of quinacridone–lignocellulose mixture became increasingly vivid as the weight ratio of the lignocellulose fibers increased and as the fiber was fibrillated. The nuclear Overhauser effect spectroscopy (NOESY)–nuclear magnetic resonance (NMR) spectrum for quinacridone–lignocellulose suspension in *d*-dimethyl sulfoxide showed several NOE cross-peaks between quinacridone and cellulose/hemicellulose, whereas no cross-peaks between quinacridone and lignin were observed. It can be concluded that cellulose and hemicellulose promote the adsorption of quinacridone on the fiber surface, whereas lignin does not interact with quinacridone, even though both are aromatic molecules. This suggests that the intermolecular interactions based on hydrogen bonding and CH–π attraction are more dominant than the π–π attraction between quinacridone and lignocellulosic fibers.

Keywords Lignocellulosic fiber, Lignocellulose, Organic pigment, Quinacridone, Aggregation inhibition, Intermolecular interaction, Gel-state NMR

*Correspondence:
Yasuko Saito
saitou.y4@aist.go.jp
[1] Research Institute for Sustainable Chemistry, National Institute of Advanced Industrial Science and Technology (AIST), Hiroshima 739-0046, Japan
[2] Sanyo Color Works, Ltd, Hyogo 670-0966, Japan

Introduction

Organic pigment molecules tend to intrinsically assemble through intermolecular interactions to form aggregates. Suppression of pigment aggregation is a problem in the coloration industry, because aggregate formation causes undesired color changes [1, 2]. Quinacridone, a widely used red–violet pigment, is prone to aggregation because of intermolecular N–H···O hydrogen bonding and π–π stacking [3]. Recently, we reported that cellulose nanofiber (NF) and chitosan NF are potential dispersant materials for quinacridone [4, 5]. Both NFs effectively adsorb quinacridone particles and suppress the aggregation of quinacridone. Gel-state nuclear magnetic resonance (NMR) spectroscopic investigations indicated the existence of an intermolecular interaction between the NFs' surface and quinacridone. The nuclear Overhauser effect spectroscopy (NOESY)–NMR analysis for the cellulose NFs and quinacridone mixture suspended in deuterated solvents, termed gel-state NMR analysis, detected cross-peaks between signals assigned to cellulose and quinacridone. This suggested that there should be hydrogen bonding between the glucose repeating unit of cellulose and the NH group of quinacridone, as well as the CH–π interaction between the CH group of cellulose and the aromatic group of quinacridone. These interactions should achieve a high quinacridone adsorption performance of the cellulose NF. As a result, the adsorption of quinacridone primary particles onto cellulose NFs is preferred to the aggregation of quinacridone primary particles, to inhibit quinacridone aggregation. In contrast, the chitosan NF was found to interact with quinacridone dominantly through hydrogen bonding between the glucosamine repeating unit of chitosan and the carbonyl group of quinacridone, as revealed by gel-state NMR. Therefore, the interaction between the components of NFs and quinacridone was important for suppressing quinacridone aggregation using polysaccharide NFs.

In our previous study, cotton powder, which consists of more than 99% cellulose, was used as a raw material for NFs with the intention of displaying the properties of cellulose. However, major cellulose NFs made from biomass, such as wood, ground pulp, kraft pulp, and agricultural residues, contain cellulose and other components such as hemicellulose and lignin [6, 7]. In bioresources, cellulose, hemicellulose, and lignin interact with each other and some of them are covalently linked [8, 9]. For example, hemicellulose is considered to coat the lignocellulose NF surface, although its distribution varies among plant species, as revealed by monitoring the enzymatic hydrolysis of lignocellulosic NFs using a quartz crystal microbalance [10]. In spruce secondary cell walls, hemicelluloses glucomannan and xylan exist close to cellulose microfibrils and lignin, as investigated using ^{13}C multidimensional solid-state NMR spectroscopy [11]. Therefore, it is assumed that hemicellulose and lignin influence the surface properties of lignocellulosic NFs and, therefore, the adsorption behavior of pigment molecules, including quinacridone. Because quinacridone is a π-conjugated planar molecule, the π–π intermolecular interaction between quinacridone and lignin is expected, potentially resulting in improved dispersion properties for quinacridone and a better color appearance than cotton-derived cellulose NFs.

In this study, the properties of lignocellulosic fibers as pigment dispersants were investigated. Two fibrillated softwood mechanical pulps were used as lignocellulosic fibers, named lignocellulose microfiber (MF) and lignocellulose NF in this paper. The adsorption of quinacridone onto lignocellulosic fiber and aggregation inhibition behavior were evaluated using scanning electron microscopy (SEM). The molecular interactions between lignocellulose and quinacridone were verified by gel-state NMR spectroscopy. The color properties of the quinacridone/lignocellulosic fibers were compared with those of pure cellulose NF. Finally, we discuss the intermolecular interactions between quinacridone and lignocellulosic fibers. In this study, we demonstrated that cellulose and hemicellulose interact well with quinacridone via hydrogen bonding and CH–π attraction, whereas lignin does not interact with quinacridone.

Experimental

Materials

Quinacridone powder (γ-form) was treated with salt milling to decrease the diameter of the primary particles. The milled quinacridone obtained was washed with water and used without drying to inhibit further aggregation. The diameter of the primary particles was approximately 60 nm, as determined using transmission electron microscopes (JEM-1011, JEOL Ltd., Tokyo, Japan). Two fibrillated softwood mechanical pulps were obtained from Daio Paper Corporation (Tokyo, Japan). The lignocellulosic fibers before and after mechanical fibrillation were named lignocellulose MF and lignocellulose NF, respectively. The composition of the lignocellulosic fibers is listed in Table 1, which shows that the main components of hemicellulose components are glucomannan and xylan, and over 30% of the wood components are lignin. The neutral carbohydrates components showed that lignocellulosic fiber contained glucomannan and xylan as hemicellulose. Deuterated dimethyl sulfoxide (DMSO-d_6) was purchased from Wako Pure Chemical Industries Ltd. (Osaka, Japan).

Table 1 Results of fraction analysis of lignocellulose MF

Neutral sugar (relative amount (%))[a]					Klason lignin	Acid soluble lignin	Ash
Arabinose	Xylose	Mannose	Galactose	Glucose	(%)	(%)	(%)
0.0	7.5 ± 0.73	17.2 ± 0.52	0.0	75.3 ± 0.44	31.2 ± 0.16	4.5 ± 0.30	1.2 ± 0.06

[a] Relative amount (sum of neutral sugar = 100%)

Characterization of lignocellulosic fibers

For Brunauer–Emmett–Teller (BET) analysis, parts of the aqueous suspension of lignocellulosic fibers were subjected to solvent exchange with *tert*-butyl alcohol and freeze-dried. Nitrogen adsorption isotherms of the dried fibers were obtained using a BELSORP-max instrument (BEL Japan, Inc., Osaka, Japan). The specific surface areas of the lignocellulosic fibers were calculated from BET plots. Chemical composition of lignocellulose MF were determined according to the procedure reported from National Renewable Energy Laboratory (NREL) with some modifications [12]. Ash content was calculated from residue after thermal treatment at 600 °C for 24 h. Klason lignin was collected as a residue after the acid hydrolysis of the dried lignocellulose MF. The amount of acid soluble lignin was determined using UV–Vis spectrum of filtrate after acid hydrolysis. The composition of the neutral carbohydrates was determined by ion chromatography after acid hydrolysis. Fourier transform infrared (FTIR) spectra of lignocellulose MF and NF were obtained on an FTTIR spectrometer Frontier (PerkinElmer Inc., MA, USA) equipped with a diamond/ZnSe attenuated total reflectance. A processing software Spectrum IR version 10.6.1 (PerkinElmer Inc., MA, USA) was used. Both spectra were normalized using absorption peak at 1317 cm^{-1}.

Adsorption quinacridone particles onto lignocellulosic fibers

Suspensions of lignocellulose MF and NF (2.0 wt%) were prepared by diluting with distilled water. A portion of the lignocellulose suspension was added to 7.9 g of the 2.5 wt% quinacridone suspension. A series of quinacridone–lignocellulose mixtures was prepared, and the weight ratios of quinacridone to the lignocellulosic fibers were adjusted to 2:1, 1:1, 1:2, 1:4, 1:9, and 1:19 (w/w). Then, distilled water was added to each suspension to increase the mass to 200 g to achieve a quinacridone concentration of 0.1 wt%. Subsequently, pigment particles and lignocellulose were dispersed for 1 min using an ultrasonic homogenizer US-150 T (NIHON SEIKI Co., Ltd., Tokyo, Japan) equipped with a 20 mm diameter probe tip at 19.5 kHz. Quinacridone water dispersion (0.1 wt%) was prepared as a control.

SEM observation

Portions of lignocellulose and quinacridone–lignocellulose aqueous suspensions were subjected to solvent exchange with *tert*-butyl alcohol and freeze-dried. Dried samples were placed on conductive tape and coated with osmium using an osmium coater (Tennant 20, Meiwafosis Co., Ltd., Tokyo, Japan) before observation. Observations were performed using field-emission SEM S-4800 (Hitachi High-Tech Corp., Tokyo, Japan). The acceleration voltage was adjusted to 1.0 kV.

NMR measurements

The NMR test sample was prepared as previously reported [4]. A portion of the quinacridone–lignocellulose NF mixture (1:9, w/w) was treated with acetone, and the precipitate was collected via filtration. This procedure was repeated twice. The collected mixture was then dried under reduced pressure at room temperature. The dried samples were cryogenically pre-ground for 30 min at 30 s intervals using a cryogenic sample crusher JFC-300 (Japan Analytical Industry Co., Ltd., Tokyo, Japan). A 30 s break was taken between each crushing process. Subsequently, further pulverization was performed by ball milling using a PULVERISETTE 7 planetary mono micro mill (Fritsch GmbH, Idar-Oberstein, Germany). A zirconium dioxide vessel and balls (ϕ5 mm) were used. The spun samples were spun at 600 rpm for 20 min in intervals with 20 min interval breaks. This process was repeated twelve times. The ball-milled samples (10 mg) were dispersed in 0.7 mL DMSO-d_6 by sonication for 6 h using an ultrasonic cleaner ASU-10 M (AS ONE Corp., Osaka, Japan). NMR spectra were recorded on a 400 MHz NMR spectrometer (Agilent Technologies, Santa Clara, CA, USA) at room temperature and 80 °C. To control the spectrometer and process the spectra, Agilent's software VnmrJ 4.2 was used. The ^{1}H, ^{13}C–^{1}H heteronuclear single quantum coherence (HSQC), and NOESY NMR were measured by Agilent standard pulse sequences 'Proton', 'Gradient HSQCAD', and 'NOESY', respectively. The DMSO central peak was used as the internal reference (δ_C/δ_H: 39.50/2.49 ppm). The contours in HSQC–NMR spectra were colored using Adobe Photoshop Element 14 (Adobe Inc., San Jose, USA).

Color measurements

To evaluate the color of quinacridone–lignocellulose aqueous suspensions, an L^* a^* b^* system was used. The color properties L^*, a^*, and b^* represent the lightness, green (−)/red (+) axis, and blue (−)/yellow (+) axis, respectively. The quinacridone–lignocellulose suspensions described above, which the concentration of quinacridone was 0.1 wt%, were used without diluting. The reflectance spectra of the suspensions were recorded using a CM 3600A spectrometer (KONICA MINOLTA, Inc., Tokyo, Japan). A standard D65 illuminant was irradiate from the side of the cell with a white calibration plate on the other side of the cell. The light path length through the dispersion was 4 mm. To detect the reflected light, the specular component included (SCI) mode and a 2° angle for a normal observer were selected. The color properties L^*, a^*, and b^* were determined from the reflectance spectra using the processing software CM-S100w (KONICA MINOLTA). All measurements were performed more than thrice for each suspension. To minimize the effects of sedimentation, the color parameters at different locations for each dispersion were measured and were averaged.

Results and discussion

Characterization of lignocellulosic fibers

The specific surface areas of lignocellulosic MF and NF was determined from BET plots of their nitrogen adsorption isotherms and were 29.5 and 78.1 m^2/g, respectively. The morphology of the freeze-dried fibers was observed by SEM. The lignocellulosic MF exhibited thick fibers with diameters of several micrometers (Fig. 1a). After mechanical treatment, the fibers with several tens to several hundred nanometers in diameter with high aspect ratio were observed, although some fibers with a micrometer in diameter also existed (Fig. 1b). The fiber after mechanical fibrillation was named lignocellulosic NF, because cellulosic fibers with nanometer diameters with high aspect ratio are called cellulose NF [13]. Fraction analysis of lignocellulosic MF is shown in Table 1. In the FTIR spectrum of lignocellulosic MF (Fig. 2a), absorption peaks of lignin were observed at 1600 cm^{-1} (C=C stretching of aromatic moiety), 1509 cm^{-1} (C=C stretching of aromatic moiety), and 1453 cm^{-1} (asymmetric bending in CH_3 of lignin), respectively [14]. In addition, adsorption peaks at 1424, 1370, 1317, 1056, 1032, and 896 cm^{-1} related to cellulose were also detected [15]. A negligible absorption around 1740 cm^{-1} suggested

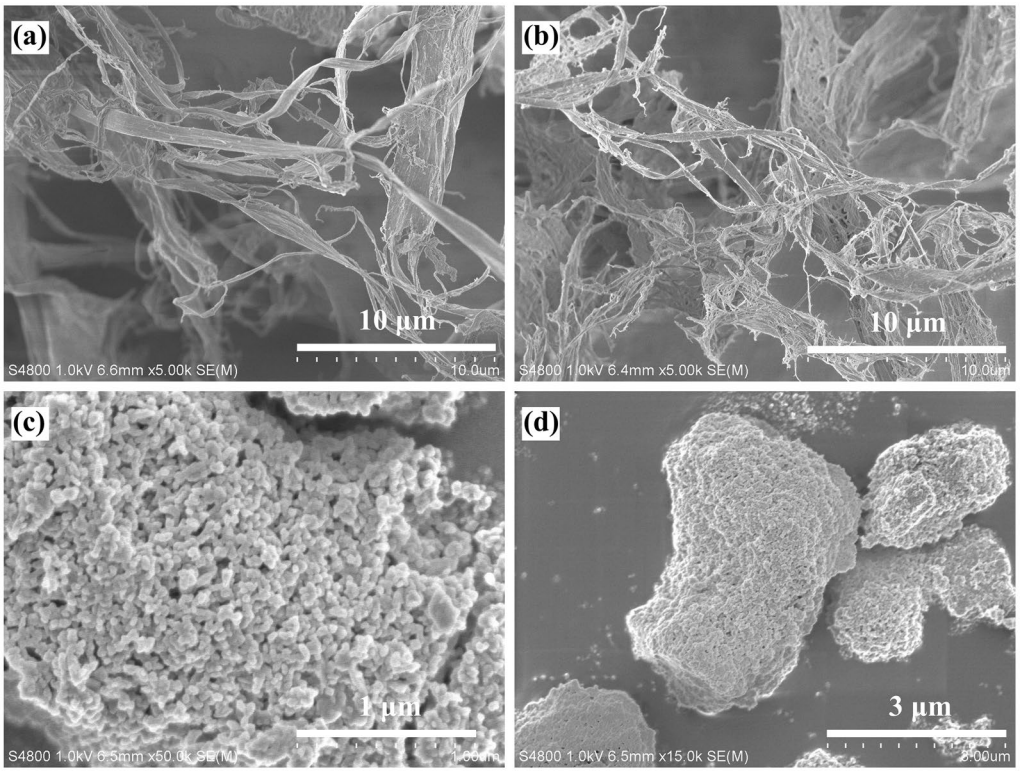

Fig. 1 SEM images of **a** lignocellulose MF, **b** lignocellulose NF, and **c** and **d** quinacridone

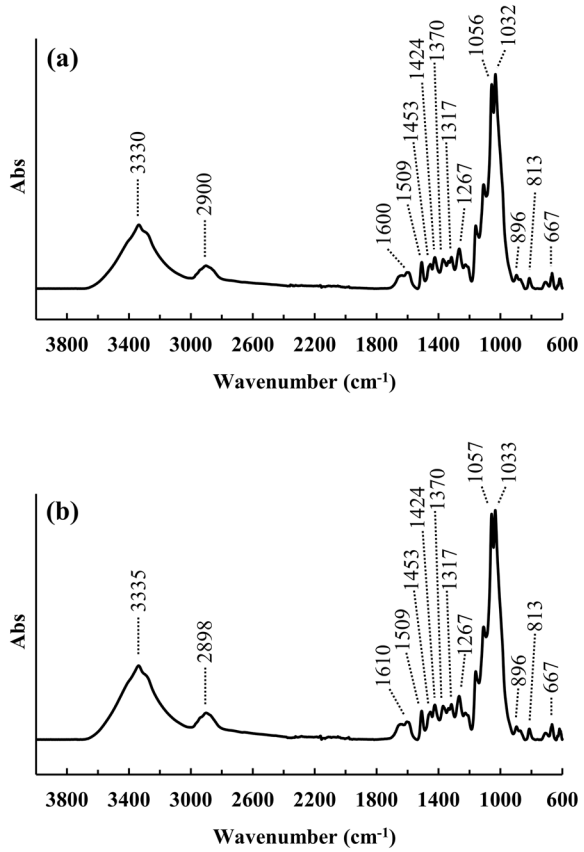

Fig. 2 FTIR spectra of, lignocellulose **a** MF and **b** NF

that lignocellulosic fibers used in this study contain little acetyl groups in glucomannan fraction [16]. The FTIR spectrum of lignocellulosic NF (Fig. 2b) was accordance with that of lignocellulosic MF, indicating the components were same before and after fibrillation.

Adsorption of quinacridone on lignocellulosic fibers

Quinacridone molecules tended to assemble and form primary particles. Because the surface energy of small primary particles is high, they aggregate into large clusters called secondary particles. The average size of the primary particles of quinacridone used in this study was 60 nm (Fig. 1c). Secondary quinacridone particles were observed in the absence of lignocellulosic fibers or additives (Fig. 1d). The quinacridone secondary particles were several micrometers in diameter.

To investigate the quinacridone aggregation inhibition behavior of lignocellulosic MF and NF, quinacridone and lignocellulose water suspensions were mixed as previously reported [5]. Figure 3 shows the morphology of freeze-dried quinacridone–lignocellulose mixtures. In the quinacridone–lignocellulose MF mixture (2:1, w/w), quinacridone secondary particles > 1 μm in diameter were observed which is indicated by 'A' in Fig. 3a. When the amount of lignocellulose MF increased to nine times that of quinacridone, quinacridone aggregation decreased; however, aggregations existed (Fig. 3b, B). In addition, the quinacridone–lignocellulose NF mixture (2:1, w/w) also contained aggregated quinacridone particles (Fig. 3c, C). However, as the amount of lignocellulose NF increased, the dispersion of the quinacridone primary particles progressed (Fig. 3d–f). Hence, the fibrillation of lignocellulose improved quinacridone aggregation inhibition ability. Few quinacridone aggregates were observed in the quinacridone–lignocellulose NF mixture (1:9, w/w). These results were similar to those obtained using cellulose NFs. Therefore, lignocellulose NF has quinacridone aggregation inhibition ability, suggesting that hemicellulose and lignin did not diminish quinacridone adsorption capacity.

NMR spectroscopy

NMR measurements of quinacridone–cellulose NF and quinacridone–chitosan NF mixtures indicated that the intermolecular interaction between quinacridone and NF was different by the chemical structure of NF constituents. Such difference was suggested to affect quinacridone aggregation inhibition property of NF [5]. Because the SEM observations suggest that lignocellulose NF adsorbed more quinacridone primary particles than lignocellulose MF, the intermolecular interaction between quinacridone and lignocellulose NF (1:9, w/w) was investigated using gel-state NMR. Gel NMR spectroscopy was originally proposed by Mansfield et al. [17] and we developed its application in the intermolecular interaction analysis of polysaccharide NFs [4]. This technique enables the analysis of insoluble samples in common NMR solvents with the advantage of solution-state NMR spectroscopy to identify the chemical compounds and evaluate intramolecular interactions.

The quinacridone–lignocellulose NF mixture was dried, cryogenically pre-ground, and ball-milled. The pulverized mixture was then dispersed in DMSO-d_6. After the suspension was treated with an ultrasonic cleaner, quinacridone–lignocellulose NF (1:9, w/w) were stably dispersed.

First, we determined the optimum temperature for NMR measurements of the quinacridone–lignocellulose NF mixture. The measurement temperature was varied in the range 23–80 °C, and the detectability and resolution of ^{1}H signals derived from quinacridone were compared. Some of the results are shown in Fig. 4. The resolution of the signals assigned to quinacridone improved with increasing measurement temperature. Accordingly, it was concluded that the spectrum measured at 80 °C had the highest resolution. In the previous study [4], ^{1}H–^{1}H

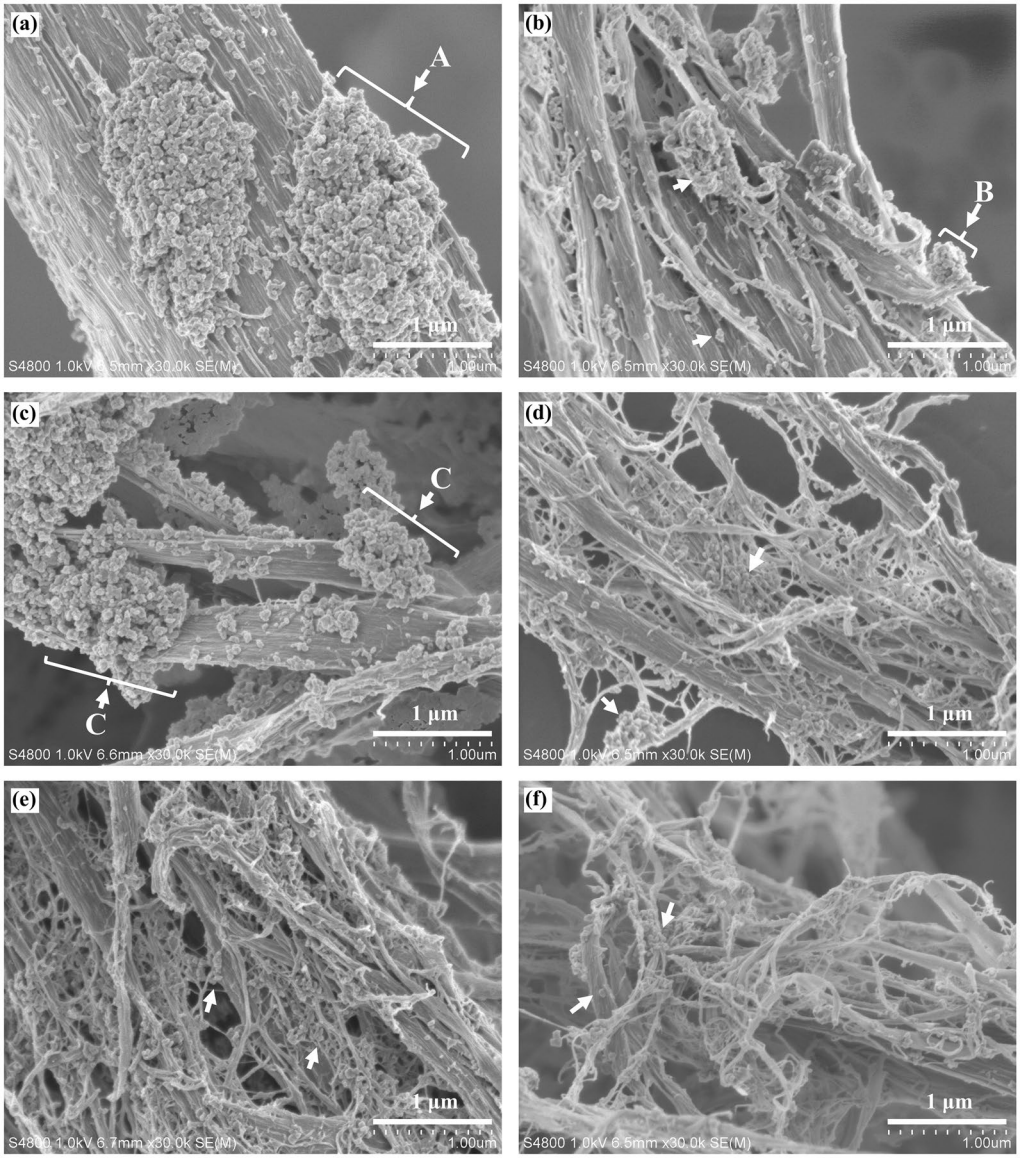

Fig. 3 SEM images of quinacridone–lignocellulosic fiber mixtures. The mixtures of quinacridone and lignocellulose MF **a** 2:1 (w/w), **b** 1:9 (w/w), and the mixtures of quinacridone and lignocellulose NF **c** 2:1 (w/w), **d** 1:1 (w/w), **e** 1:4 (w/w), and **f** 1:9 (w/w). Arrows indicate quinacridone particles

NOESY–NMR spectrum of quinacridone–cellulose NF mixture suggested the interaction between aromatic moiety of quinacridone and H3 and H4 of the glucose repeating unit of cellulose, denoted as G3 and G4. However, the possibility of the interaction between quinacridone and water could not be excluded, because ^{1}H signals assigned to G3, G4, and water were overlapped. Those signals detected at approximately $\delta = 3.0$ ppm at 30 °C. In Fig. 4, as the temperature increased, the signal of water shifted to upper magnetic field, while the chemical shifts of G3 and G4 were almost same irrespective of temperature. Finally, at 80 °C, the signal of water became distinguishable from the signals derived from G3 and G4 of cellulose, successfully indicating that the interaction between quinacridone and cellulose. From these results, the NMR experiments were conducted at 80 °C.

The HSQC–NMR spectrum of the quinacridone and lignocellulose NF mixture is shown in Fig. 5. Cross-peaks assigned to quinacridone, cellulose (glucose unit), mannan (mannose unit), xylan (xylose unit), and lignin (β-O-4 structure) were detected. Each peak was identified by comparing with the NMR spectra in the literature [18–22]. The correlation peaks assigned to the C5/H5 of glucose and mannose were not detected under the

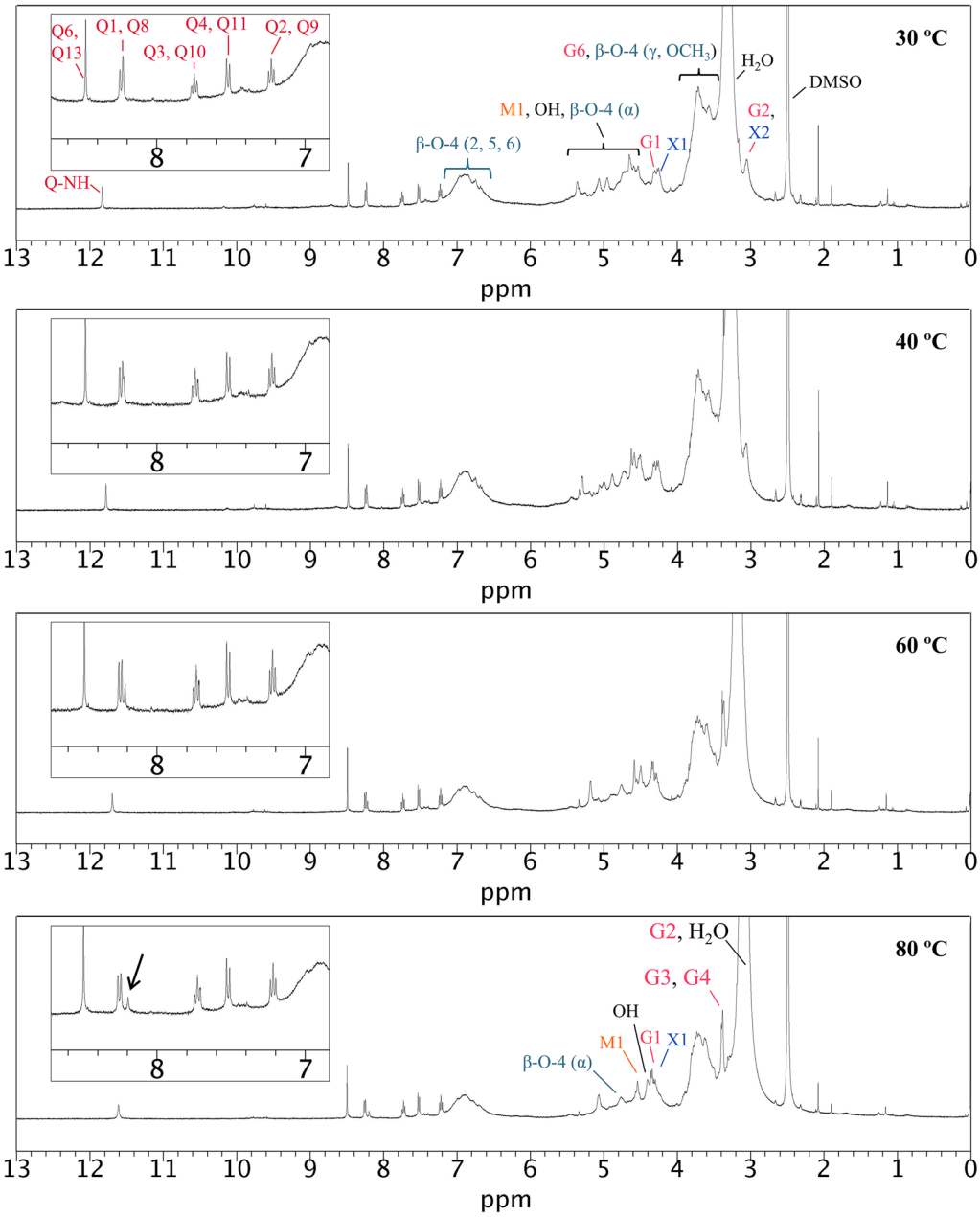

Fig. 4 Effect of measurement temperature on gel-state ^{1}H NMR spectra for quinacridone–lignocellulose NF (1/9, w/w). The test sample was suspended in DMSO-d_6. G, X, and M represent glucose, xylose, and mannose units, and β-O-4 denote β-O-4 unit of lignin. The chemical structure of each unit shows in Fig. 5

measurement conditions. The signals owing to quinacridone, except for NH, were detected at almost the same chemical shifts as in a previous study [4]. The chemical shifts of quinacridone, polysaccharides, and lignin barely changed regardless of the temperature increase, except for the NH proton of quinacridone. Although the chemical shift of the NH group of quinacridone was changed from 11.9 ppm at 23 °C to 11.6 ppm at 80 °C (Fig. 4), this may be independent of lignocellulose NF, because similar behavior was observed when measuring the dispersion of quinacridone alone. Therefore, a NOESY experiment of the quinacridone–lignocellulose NF mixture was conducted to investigate the intermolecular interactions between quinacridone and lignocellulose.

Next, ^{1}H–^{1}H NOESY–NMR measurements of quinacridone–lignocellulose NF were performed. The

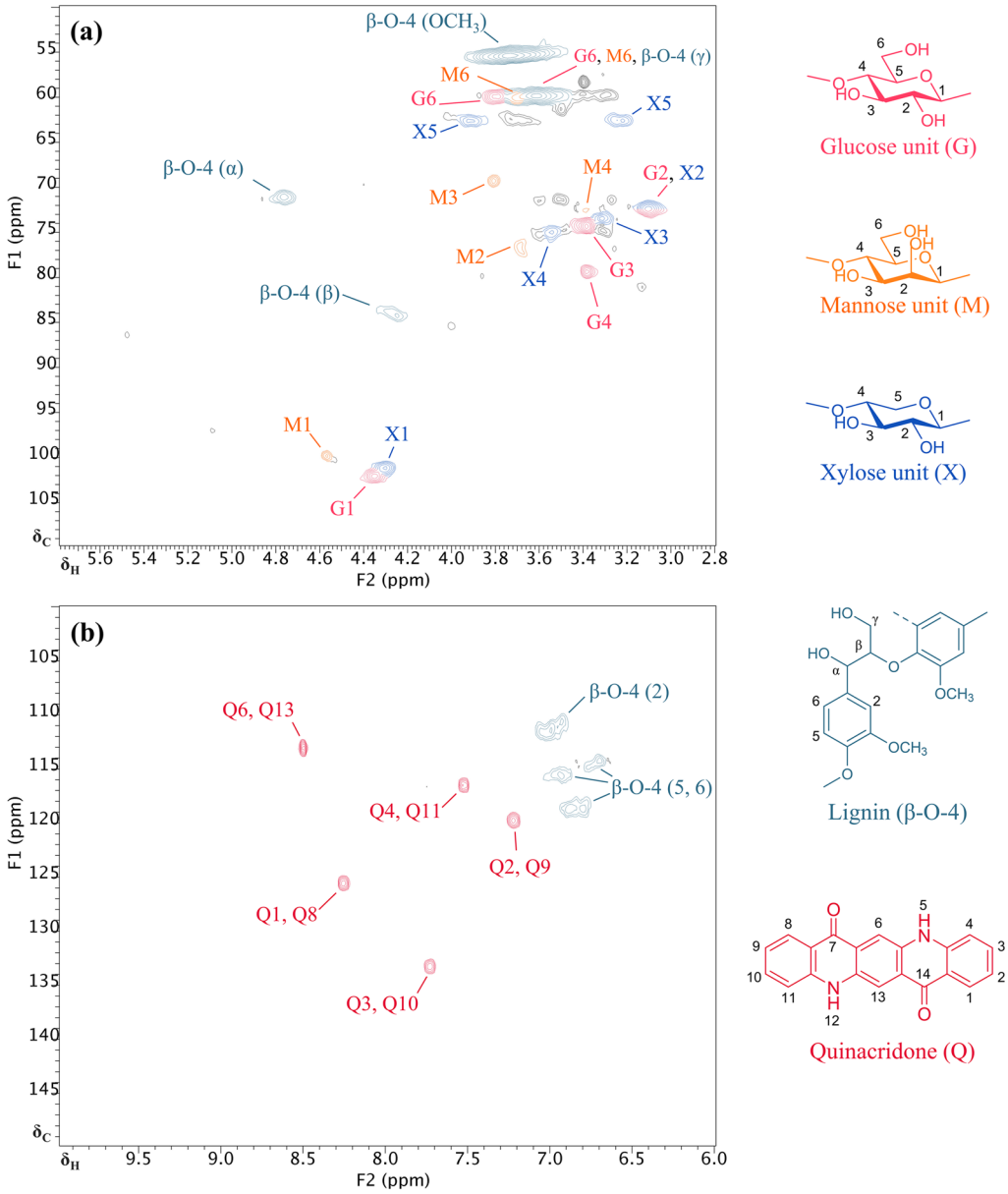

Fig. 5 HSQC–NMR spectra of quinacridone and lignocellulose NF (1/9, w/w). **a** Aliphatic region and **b** aromatic region

cross-peaks detected in this experiment suggest that protons exist closer than 5 Å or exchange [23]. A different lot of the quinacridone–lignocellulose NF mixture was used in the NOESY experiment after confirming that a same ^{1}H NMR spectrum as in Fig. 4 was obtained. Similar to the quinacridone–cellulose NF mixture, cross-peaks between the signals of quinacridone and G3 or G4 cellulose were observed (region A of Figs. 6 and 7). In addition, there were signal cross-peaks at approximately 8.2–8.3 ppm and 4.3–4.6 ppm (region B of Figs. 6 and 7). In the 4.3–4.6 ppm region, H1 of mannose was detected in the HSQC–NMR spectrum (Fig. 5). Therefore, glucomannan may exist closely to quinacridone particles. In addition, although the peak area was small, the cross-peak between Q1, 8 and each H1 of glucose and xylose were observed. These results suggested that cellulose and hemicellulose may have contributed to the adsorption of quinacridone particles. They are considered to interact with quinacridone at several positions via CH–π interactions and hydrogen bonding. Unexpectedly, no apparent cross-peaks between the aromatic moieties of lignin and quinacridone were observed. This result indicated that

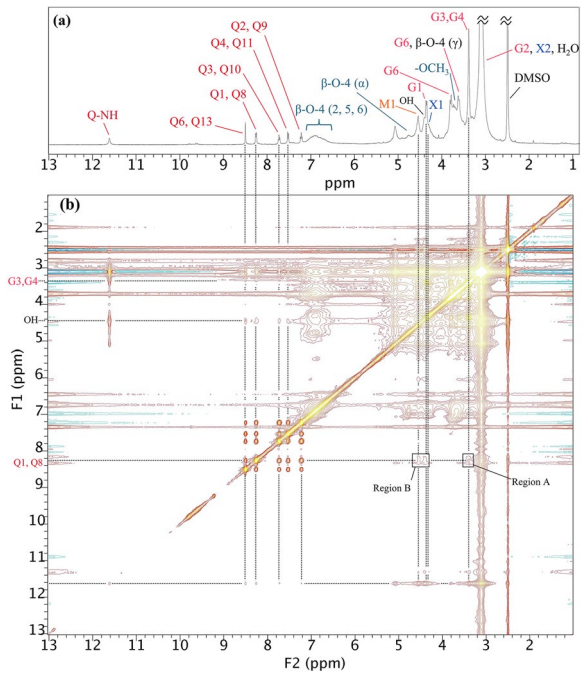

Fig. 6 **a** ^{1}H and **b** NOESY–NMR spectra of quinacridone and lignocellulose NF (1/9, w/w)

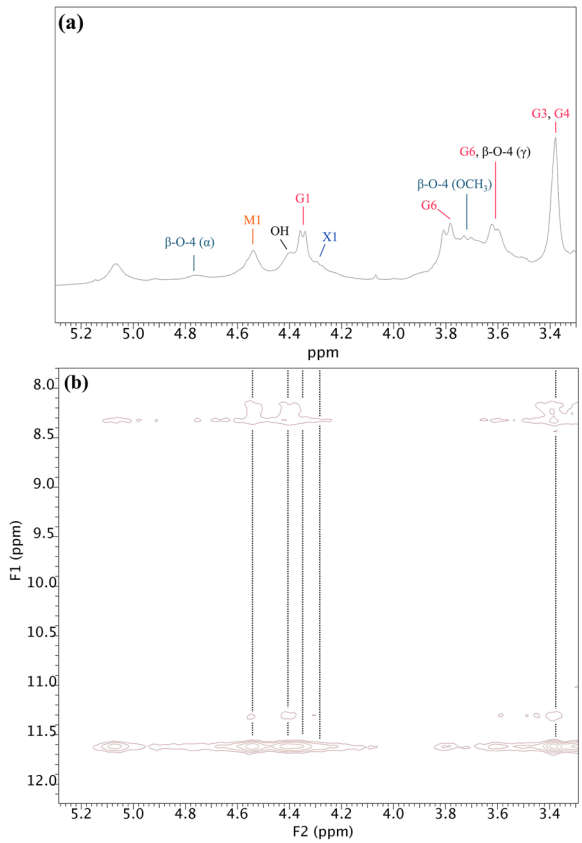

Fig. 7 Expanded figures of **a** ^{1}H and **b** NOESY–NMR spectra of quinacridone and lignocellulose NF (1/9, w/w)

there may be few intermolecular interactions between the aromatic moieties and quinacridone via the π–π interactions. In addition, lignin is a steric and amorphous phenolic polymer, whereas quinacridone has a planar structure. Thus, one possible reason for the low affinity between lignin and quinacridone is the steric hindrance.

Cellulose, chitosan, and lignocellulose interacted strongly with quinacridone; however, their mechanisms were different. Comparing the interaction between NFs and quinacridone, which has been investigated, there may be CH–π interactions and hydrogen bonding between quinacridone and the glucose, mannose, and xylose units of polysaccharides. However, the π–π interactions between lignin and quinacridone can be negligible. Therefore, cellulose and lignocellulose NF should adsorb quinacridone induced by CH–π interactions and hydrogen bonding. Unlike cellulosic fibers, chitosan NFs interact with quinacridone via hydrogen bonding through the NH group of quinacridone.

Color measurement

The quinacridone and quinacridone–lignocellulosic NF dispersions showed different hue, although the quinacridone concentration was constant (Fig. 8). The color of quinacridone–cellulose aqueous suspensions depends on various conditions, such as quinacridone concentration and aggregate formation, the weight amount of cellulosic fibers, and degree of cellulosic fiber fibrillation [5, 24]. In several cases, it was indicated that parameters L^* and a^* increased, whereas parameter b^* decreased when quinacridone aggregation

Fig. 8 Photographs of quinacridone aqueous dispersion. Left: quinacridone dispersion and right: quinacridone–lignocellulosic NF mixture (1:19, w/w). In both dispersions, the concentration of quinacridone was 0.1 wt%

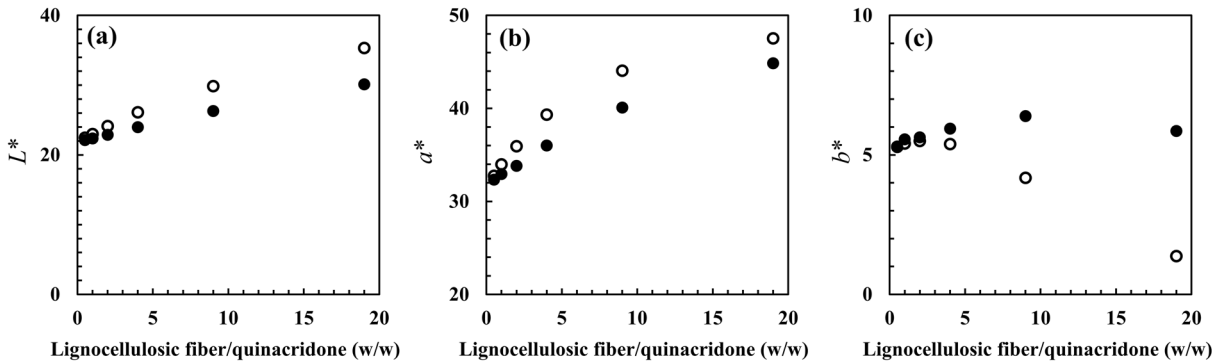

Fig. 9 Influence of lignocellulose on color parameters. **a** L^* (lightness), **b** a^* (green (−)/red (+) axis), and **c** b^* (blue (−)/yellow (+) axis). Closed circle: lignocellulose MF and open circle: lignocellulose NF

was disassembled by treatment with an acrylic polymer dispersant, when compared to the color of the quinacridone aqueous suspension [5]. Figure 9 shows the influence of lignocellulosic fibers on the color parameters of the quinacridone aqueous dispersion. The values of parameters L^*, a^*, and b^* of the 0.1 wt% quinacridone aqueous suspension measured using the same color spectrometer were 20.99, 31.63, and 4.38, respectively [5]. These values varied with the addition of lignocellulosic fibers, although the concentration of quinacridone was the same. The color parameters, L^* and a^*, increased as the weight ratio of lignocellulose MF increased. This indicated that the dispersion color became brighter. The parameters L^* and a^* increased further when quinacridone was treated with lignocellulose NF, as compared to lignocellulose MF. Moreover, the b^* value of quinacridone–lignocellulose NF aqueous suspensions decreased as the lignocellulose NF increased. However, the b^* value of quinacridone–lignocellulose MF was practically equal irrespective of the amount of lignocellulose. This result was in accordance with the quinacridone aggregation inhibition observed using SEM. Therefore, as is the case of cellulose NF [24], it was suggested that the addition of lignocellulose NF suppressed quinacridone aggregation and can improve the color strength of quinacridone. When quinacridone was treated with 19 times more lignocellulose NF, the color parameters L^*, a^*, and b^* of the suspension were 35.33, 47.52, and 1.37, respectively. Except for b^*, these values were nearly equal to the color parameters of quinacridone–cellulose NF mixture (1:19, w/w), which were calculated to be 34.67, 46.45, and − 1.76 [5]. The reason for the difference in parameter b^* may be related to the difference between the color of the mechanical pulp and cotton cellulose. Overall, the properties of the lignocellulose NF as a dispersant for quinacridone are expected to be comparable to those of cellulose NF, which consists almost entirely of cellulose.

Conclusions

The influence of hemicellulose and lignin on the adsorption of quinacridone on lignocellulosic fibers was investigated. Fibrillated mechanical pulps containing cellulose, lignin, and hemicellulose were used. Lignin and hemicellulose did not affect quinacridone adsorption onto cellulose fibers. Furthermore, lignocellulose NFs exhibited quinacridone aggregation inhibitory properties similar to those of cellulose NF without lignin and hemicellulose. In addition to cellulose fibers, fibrillation of lignocellulose improved the inhibition of quinacridone aggregation. The gel-state NMR analyses of quinacridone–lignocellulose NF indicated that xylan, glucomannan, and cellulose interacted with quinacridone, whereas lignin hardly interacted with quinacridone. In conclusion, lignocellulose NFs are expected to be potential materials for quinacridone dispersants as well as pure cellulose NFs without hemicellulose and lignin.

Abbreviations

NF	Nanofiber
SEM	Scanning electron microscopy
NOESY	Nuclear Overhauser effect spectroscopy
NMR	Nuclear magnetic resonance
NOE	Nuclear Overhauser effect
MF	Microfiber
DMSO-d_6	Deuterated dimethyl sulfoxide
BET	Brunauer–Emmett–Teller
NREL	National Renewable Energy Laboratory
FTIR	Fourier transform infrared
HSQC	Heteronuclear single quantum coherence
SCI	Specular component included

Acknowledgements

The authors express their gratitude to Daio Paper Corporation for kindly providing the fibrillated mechanical pulps.

Author contributions
YS designed this study and was mainly responsible for the preparation of quinacridone–lignocellulose mixture, SEM observations, and preparation of the paper. KS contributed to the discussion of the obtained results and supervised the final manuscript. YT contributed to the acquisition and interpretation of NMR data. NH participated in planning the experimental methods and contributed to color measurements. TE designed the research and supervised the final manuscript. All authors read and approved the final manuscript.

Funding
No funding.

Availability of data and materials
The data sets used and/or analyzed during the current study are available from the corresponding author on reasonable request.

Declarations

Competing interests
The authors declare that they have no competing interests.

Received: 3 January 2023 Accepted: 21 April 2023
Published online: 18 May 2023

References

1. Hao Z, Iqbal A (1997) Some aspects of organic pigments. Chem Soc Rev 26:203–213. https://doi.org/10.1039/cs9972600203
2. Skillas G, Agashe N, Kohls DJ, Ilavsky J, Jemian P, Clapp L, Schwartz RJ, Beaucage G (2002) Relation of the fractal structure of organic pigments to their performance. J Appl Phys 91:6120–6124. https://doi.org/10.1063/1.1466524
3. Chen P, Liu GJ, Wang Y, Zhang SXA (2016) A stable aggregate system of silyl ether substituted quinacridone and its aggregation-state changes induced by fluoride-ions: inspiration for a dual guaranteed strategy for probe design. RSC Adv 6:25986–25991. https://doi.org/10.1039/c6ra01487a
4. Saito Y, Iwamoto S, Hontama N, Tanaka Y, Endo T (2020) Dispersion of quinacridone pigments using cellulose nanofibers promoted by CH–π interactions and hydrogen bonds. Cellulose 27:3153–3165. https://doi.org/10.1007/s10570-020-02987-0
5. Saito Y, Iwamoto S, Tanaka Y, Hontama N, Endo T (2021) Suppressing aggregation of quinacridone pigment and improving its color strength by using chitosan nanofibers. Carbohydr Polym 255:117365. https://doi.org/10.1016/j.carbpol.2020.117365
6. Isogai A (2013) Wood nanocelluloses: fundamentals and applications as new bio-based nanomaterials. J Wood Sci 59:449–459. https://doi.org/10.1007/s10086-013-1365-z
7. Pennells J, Godwin ID, Amiralian N, Martin DJ (2020) Trends in the production of cellulose nanofibers from non-wood sources. Cellulose 27:575–593. https://doi.org/10.1007/s10570-019-02828-9
8. Terrett OM, Dupree P (2019) Covalent interactions between lignin and hemicelluloses in plant secondary cell walls. Curr Opin Biotechnol 56:97–104. https://doi.org/10.1016/j.copbio.2018.10.010
9. Nishimura H, Kamiya A, Nagata T, Katahira M, Watanabe T (2018) Direct evidence for α ether linkage between lignin and carbohydrates in wood cell walls. Sci Rep 8:6538. https://doi.org/10.1038/s41598-018-24328-9
10. Kumagai A, Endo T (2018) Comparison of the surface constitutions of hemicelluloses on lignocellulosic nanofibers prepared from softwood and hardwood. Cellulose 25:3885–3897. https://doi.org/10.1007/s10570-018-1861-9
11. Terrett OM, Lyczakowski JJ, Yu L, Iuga D, Franks WT, Brown SP, Dupree R, Dupree P (2019) Molecular architecture of softwood revealed by solid-state NMR. Nat Commun 10:4978. https://doi.org/10.1038/s41467-019-12979-9
12. Sluiter A, Hames B, Ruiz R, Scarlata C, Sluiter J, Templeton D, Crocker D. Determination of structural carbohydrates and lignin in biomass. NREL Tech Rep NREL/TP-510-42618. 2011.
13. Isogai A (2015) Structural characterization and modiications of surface-oxidized cellulose nanoiber. J Jpn Pet Inst 58:365–375. https://doi.org/10.1627/jpi.58.365
14. Colom X, Carrillo F, Nogués F, Garriga P (2003) Structural analysis of photodegraded wood by means of FTIR spectroscopy. Polym Degrad Stab 80:543–549. https://doi.org/10.1016/S0141-3910(03)00051-X
15. Colom X, Carrillo F (2002) Crystallinity changes in lyocell and viscose-type fibres by caustic treatment. Eur Polym J 38:2225–2230. https://doi.org/10.1016/S0014-3057(02)00132-5
16. Ando D, Nakatsubo F, Yano H (2017) Acetylation of ground pulp: Monitoring acetylation via HSQC-NMR spectroscopy. ACS Sustain Chem Eng 5:1755–1762. https://doi.org/10.1021/acssuschemeng.6b02518
17. Mansfield SD, Kim H, Lu F, Ralph J (2012) Whole plant cell wall characterization using solution-state 2D NMR. Nat Protoc 7:1579–1589. https://doi.org/10.1038/nprot.2012.064
18. Kim H, Ralph J (2010) Solution-state 2D NMR of ball-milled plant cell wall gels in DMSO-d_6/pyridine-d_5. Org Biomol Chem 8:576–591. https://doi.org/10.1039/b916070a
19. Kim H, Ralph J (2014) A gel-state 2D-NMR method for plant cell wall profiling and analysis: a model study with the amorphous cellulose and xylan from ball-milled cotton linters. RSC Adv 4:7549–7560. https://doi.org/10.1039/c3ra46338a
20. Du X, Pérez-Boada M, Fernández C, Rencoret J, del Río JC, Jiménez-Barbero J, Li J, Gutiérrez A, Martínez AT (2014) Analysis of lignin–carbohydrate and lignin–lignin linkages after hydrolase treatment of xylan–lignin, glucomannan–lignin and glucan–lignin complexes from spruce wood. Planta 239:1079–1090. https://doi.org/10.1007/s00425-014-2037-y
21. Sytnyk M, Głowacki ED, Yakunin S, Voss G, Schöfberger W, Kriegner D, Stangl J, Trotta R, Gollner C, Tollabimazraehno S, Romanazzi G, Bozkurt Z, Havlicek M, Sariciftci NS, Heiss W (2014) Hydrogen-bonded organic semiconductor micro- and nanocrystals: from colloidal syntheses to (opto-)electronic devices. J Am Chem Soc 136:16522–16532. https://doi.org/10.1021/ja5073965
22. Holding AJ, Mäkelä V, Tolonen L, Sixta H, Kilpeläinen I, King AWT (2016) Solution-state one- and two-dimensional NMR spectroscopy of high-molecular-weight cellulose. Chemsuschem 9:880–892. https://doi.org/10.1002/cssc.201501511
23. Lee S, Kim Y (1999) Solution structure of neuromedin B by ^{1}H nuclear magnetic resonance spectroscopy. FEBS Lett 460:263–269. https://doi.org/10.1016/S0014-5793(99)01346-0
24. Saito Y, Hontama N, Tanaka Y, Endo T (2022) Effect of fibrillation on the ability of cellulose fibers to suppress the aggregation of quinacridone. Cellul Chem Technol 56:861–872. https://doi.org/10.35812/CelluloseChemTechnol.2022.56.77

Publisher's Note